

Inhibition of cell migration and invasion mediated by the TAT-RasGAP_{317–326} peptide requires the DLC1 tumor suppressor

D Barras¹, G Lorusso², C Rüegg² and C Widmann¹

TAT-RasGAP_{317–326}, a peptide corresponding to the 317–326 sequence of p120 RasGAP coupled with a cell-permeable TAT-derived peptide, sensitizes the death response of various tumor cells to several anticancer treatments. We now report that this peptide is also able to increase cell adherence, prevent cell migration and inhibit matrix invasion. This is accompanied by a marked modification of the actin cytoskeleton and focal adhesion redistribution. Interestingly, integrins and the small Rho GTP-binding protein, which are well-characterized proteins modulating actin fibers, adhesion and migration, do not appear to be required for the pro-adhesive properties of TAT-RasGAP_{317–326}. In contrast, deleted in liver cancer-1, a tumor suppressor protein, the expression of which is often deregulated in cancer cells, was found to be required for TAT-RasGAP_{317–326} to promote cell adherence and inhibit migration. These results show that TAT-RasGAP_{317–326}, besides its ability to favor tumor cell death, hampers cell migration and invasion.

Keywords: RasGAP; DLC1; adhesion; migration; invasion; peptide

INTRODUCTION

Cancer is the second leading cause of mortality worldwide.¹ A hallmark of tumor cells is their ability to acquire an invasive phenotype and metastasize from the primary tumor.² Metastasis accounts for more than 90% of cancer-related death.^{1,2} Metastatic dissemination begins with a cellular reprogramming that allows tumor cells to escape from the primary tumor to undertake a long migration journey through tissues and in the vascular and lymphatic circulation.^{3,4} Metastatic cells are characterized by their ability to degrade the extracellular matrix at the primary site and the new colonization site and to undergo intravasation and extravasation into or from the blood and/or lymph vessels.⁵ Although the molecular events during the metastatic cascade are now relatively well understood, there are no tools yet to effectively inhibit the critical steps of the metastatic cascade and, eventually, metastasis formation.⁶

A hallmark of metastatic progression and invasiveness is increased cell motility.^{7,8} Cell migration is a complex multistep and spatiotemporally organized process. It involves the integration of signals that define cell polarity, dynamic remodeling of cytoskeleton and focal adhesion (FA) structures as well as the regulation of the adhesive interaction with the extracellular environment.⁸ FAs are structures that link the exterior of the cell to the cytoskeleton through integrin transmembrane proteins. On the one hand, FAs allow the cells to anchor on its extracellular matrix and on the other hand they modulate various signaling events involved in cell migration.⁹ Small GTPases of the Rho family, in particular RhoA, Rac1 and Cdc42, are typically triggered by integrin engagement and finely coordinate cell migration at all levels.¹⁰ For example, in addition to their central function on actin dynamics regulation, Rac1 and RhoA trigger FA formation and maturation, respectively.¹¹ Any impairment in these steps can result in an inefficient motility and therefore can

compromise metastatic progression. From a therapeutic point of view, inhibiting cell migration is a logical approach for the development of anti-metastatic drugs as it is an early event in metastatic progression.

Dysregulation of pathways regulating actin cytoskeleton dynamics and cell migration is often required for cancer cell to attain their full oncogenic potential.⁷ This can be so crucial for tumor development that some proteins modulating these pathways are in fact tumor suppressors, such as neurofibromatosis type-2 (NF2)¹² and adenomatous polyposis coli (APC).¹³ One other such tumor suppressor is deleted in liver cancer-1 (DLC1), a RhoGAP protein acting on Rho and Cdc42.¹⁴ DLC1 is mutated almost as often as p53 suggesting that it is a major player during cancer progression.¹⁵ Its reintroduction in DLC1-negative cancer cells was reported to inhibit their tumorigenicity and invasive behavior in a Rho-dependent and Rho-independent manner.¹⁶

The Rasa1 gene product p120 RasGAP (from now on referred to as RasGAP) is a negative modulator of the Ras small GTPase. RasGAP can also interact with a large number of other proteins via proline-rich, Src homology (SH), pleckstrin homology and C2 domains.¹⁷ We previously reported that full cleavage of RasGAP by caspase-3 leads to the generation of fragment N2 (RasGAP_{158–455}) that efficiently and specifically sensitizes cancer cells to a panel of anticancer therapy-induced cell death.¹⁸ The shortest region responsible for this effect resides in a 10-amino-acid sequence (RasGAP_{317–326}) within the SH3 domain.¹⁹ TAT-RasGAP_{317–326} corresponds to this sequence hooked to a cell-permeable TAT-derived peptide and synthesized with D-amino acids. TAT-RasGAP_{317–326} sensitizes a variety of tumor cells to genotoxin- and photodynamic therapy-induced death, both *in vitro* and *in vivo*.^{19–22} Importantly, it does not affect normal cells.^{19,21} In the present report, we show that TAT-RasGAP_{317–326} increases cell

¹Department of Physiology, University of Lausanne, Lausanne, Switzerland and ²Department of Medicine, University of Fribourg, Fribourg, Switzerland. Correspondence: Professor C Widmann, Department of Physiology, University of Lausanne, Bugnon 7, Lausanne, 1005, Vaud, Switzerland. E-mail: Christian.Widmann@unil.ch

adhesiveness and inhibits cell migration and invasion in a DLC1-dependent manner.

RESULTS

TAT-RasGAP₃₁₇₋₃₂₆ increases cell adhesiveness

By serendipity, we discovered that TAT-RasGAP₃₁₇₋₃₂₆ has a marked effect on cell adhesion to their substratum. Incubation of the U2OS human osteosarcoma cell line with TAT-RasGAP₃₁₇₋₃₂₆, but not with the TAT cell-permeable sequence alone, rendered it resistant to cell detachment by trypsin/EDTA in a time-dependent manner (Figure 1a). Three hours after incubation with the RasGAP-derived peptide, approximately 50% of the cells became resistant to detachment. The percentage of non-detachable cells increased to 90% after 8 h of treatment. The TAT-RasGAP₃₁₇₋₃₂₆-induced resistance to trypsin/EDTA was also observed in seven other cancer and non-cancer cell lines (Figure 1b). This phenotype was found to be reversible 4–6 h following removal of the peptide (Figure 1c). TAT-RasGAP₃₁₇₋₃₂₆ rendered U2OS cells resistant not only to trypsin-mediated detachment but also to EDTA-mediated

detachment (Figure 1d). This indicates that the mechanism allowing TAT-RasGAP₃₁₇₋₃₂₆ to block cell detachment is not due to a potential inhibitory activity on trypsin. An adhesion assay was further performed to evaluate the effect of TAT-RasGAP₃₁₇₋₃₂₆ on the adhesion speed (Figure 1e and Supplementary Figure S1A). It revealed that the RasGAP-peptide was not only negatively impinging on detachment but also significantly increased the cell adhesion rate. Although the TAT peptide alone induced a statistically significant higher adhesion speed over untreated cells, TAT-RasGAP₃₁₇₋₃₂₆ stimulated an even faster cell adhesion rate. Of note, this adhesion was already detectable 30 min after the addition of the peptide, but at this time point the cells have not yet acquired their ability to resist trypsin-mediated detachment (see Supplementary Figure S1B). TAT-RasGAP₃₁₇₋₃₂₆-treated cells displayed a spread phenotype in comparison with TAT and untreated cells (Supplementary Figure S1C). The increase in cell adhesion was confirmed using a flow-mediated detachment assay. Untreated and TAT-treated HeLa cells were detachable by a strong (400 μ l/s) and by a weaker (120 μ l/s) flow. In contrast, although

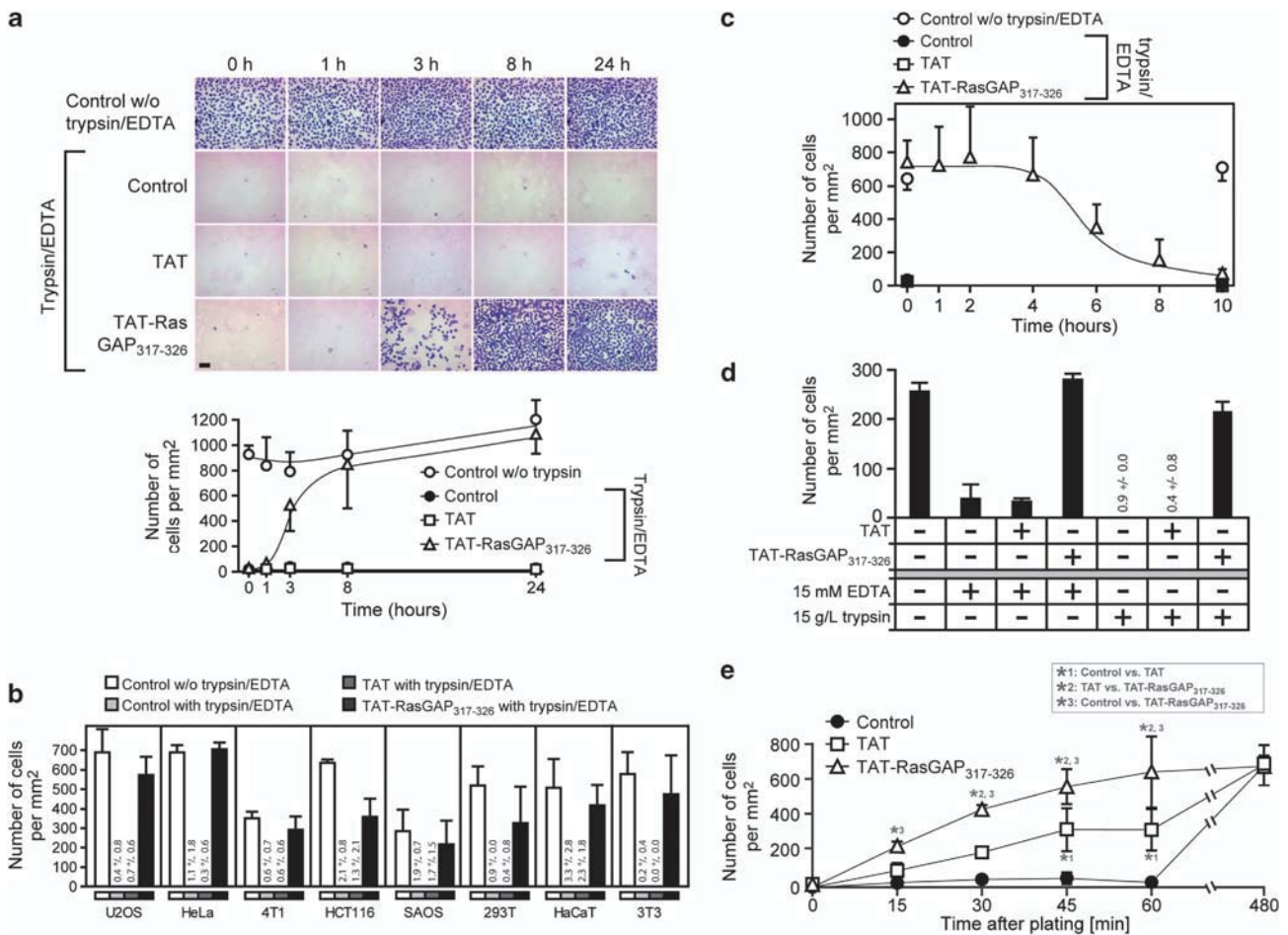


Figure 1. TAT-RasGAP₃₁₇₋₃₂₆ induces cell adhesion. **(a)** U2OS cells were treated or not for the indicated periods of time with 20 μ M TAT or TAT-RasGAP₃₁₇₋₃₂₆ and were subjected to a trypsin-based detachment assay. Representative images of the cells remaining attached to the plates after trypsin treatment are shown on top of the panel. Scale bar: 100 μ m. **(b)** The indicated cell lines were left untreated or incubated for 8 h with 20 μ M TAT or TAT-RasGAP₃₁₇₋₃₂₆, and then subjected to a trypsin-based detachment assay. Values too low to be seen on the figure graphs are shown literally. **(c)** Reversibility of the trypsin-mediated detachment induced by TAT-RasGAP₃₁₇₋₃₂₆. U2OS cells were left untreated or incubated during 24 h with 20 μ M TAT or TAT-RasGAP₃₁₇₋₃₂₆. The cells were then washed twice with phosphate-buffered saline and further incubated for the indicated periods of time in a fresh culture medium, followed by a trypsin-based detachment assay. **(d)** TAT-RasGAP₃₁₇₋₃₂₆ prevents EDTA-only- and trypsin-only-mediated cell detachment. U2OS cells were treated for 8 h with 20 μ M TAT, TAT-RasGAP₃₁₇₋₃₂₆ or left untreated. The cells were then subjected to an EDTA- and trypsin-based detachment assay ($n = 4$ independent experiments). Values too low to be seen on the figure graphs are shown literally. **(e)** U2OS cells were subjected to an adhesion assay in presence of 20 μ M TAT or TAT-RasGAP₃₁₇₋₃₂₆ or without treatment (the statistical significance of the observed differences was assessed by one-way ANOVA).

TAT-RasGAP₃₁₇₋₃₂₆-treated cells were detachable by the strong flow, they remained adherent in the presence of the 120 $\mu\text{l/s}$ flow (Figure 2). These results indicate that TAT-RasGAP₃₁₇₋₃₂₆ progressively increases cell adhesiveness, and this is likely to be the cause of their resistance to cell detachment.

TAT-RasGAP₃₁₇₋₃₂₆ acts from within the cell

To start defining the mechanisms by which TAT-RasGAP₃₁₇₋₃₂₆ affects cell adhesion, we assessed the possibility that TAT-RasGAP₃₁₇₋₃₂₆ acts from the outside of the cells to induce its effect on cell adhesion. The RasGAP₃₁₇₋₃₂₆ peptide without the TAT cell-permeable sequence, which is therefore unable to efficiently penetrate cells, was not capable to confer resistance to detachment (Supplementary Figure S2A) and to increase the adhesion rate (Supplementary Figure S2B). Adhesiveness was also increased when TAT was replaced with another cell-permeable sequence, R9, a peptide composed of nine arginine residues (Supplementary Figure S2A), indicating that the nature of the cell-permeable moiety attached to the RasGAP₃₁₇₋₃₂₆ sequence does not contribute to its activity on cell adhesion. In addition, transfection of 293T cells with a plasmid encoding the RasGAP₃₁₇₋₃₂₆ sequence rendered cells resistant to trypsin-

mediated detachment (Supplementary Figure S2C), demonstrating that cells can increase their adherence if they synthesize their own RasGAP₃₁₇₋₃₂₆ peptide. Interestingly, transfection of a plasmid-encoding fragment N2 (RasGAP₁₅₈₋₄₅₅), the parental RasGAP-derived fragment generated by caspase-3 in apoptotic cells,^{18,23} also rendered cells resistant to detachment (Supplementary Figure S2C). This indicates that the peptide can be part of a larger polypeptide and still exerts its detachment resistance activity. These data provide new insights of a potential physiological function of fragment N2 that is generated upon high caspase-3 activity.¹⁸ Taken together, these results suggest that TAT-RasGAP₃₁₇₋₃₂₆ triggers intracellular signaling pathways regulating cell adhesion.

TAT-RasGAP₃₁₇₋₃₂₆ mediates increased cell adherence through posttranslational effects

Next, the requirement of transcription and translation for the capacity of TAT-RasGAP₃₁₇₋₃₂₆ to increase cell adhesion was evaluated. U2OS cells were treated with actinomycin D, to block transcription, or with cycloheximide, to block translation, and were then subjected to a trypsin-mediated detachment assay (Supplementary Figure S3A). These drugs efficiently inhibited transcription and translation as assessed by the disappearance of the short-lived c-Myc protein (Supplementary Figure S3A). In these conditions, TAT-RasGAP₃₁₇₋₃₂₆ was still able to increase adherence, indicating that the peptide acts posttranslationally. The involvement of the proteasome was then tested. As shown in Supplementary Figure S3B (upper graph), the MG-132 proteasome inhibitor did not affect the capacity of TAT-RasGAP₃₁₇₋₃₂₆ to prevent cell detachment despite being able to inhibit cycloheximide-induced c-Myc degradation (Supplementary Figure S3B; lower blot). The observation that staurosporine, a compound able to inhibit ~90% of all kinases,²⁴ did not affect TAT-RasGAP₃₁₇₋₃₂₆-induced increased adhesiveness (Supplementary Figure S3C) indicates that most kinases are not mediating the effect of the RasGAP-derived peptide. The RasGAP SH3 domain that harbors the RasGAP₃₁₇₋₃₂₆ sequence has the potential to dimerize²⁵ raising the possibility that TAT-RasGAP₃₁₇₋₃₂₆ interacts with RasGAP or RasGAP-derived fragments and that such an interaction is required for the peptide to render cells resistant to detachment. However, RasGAP knockout mouse embryonic fibroblasts (MEFs) became resistant to trypsin-mediated detachment when incubated with TAT-RasGAP₃₁₇₋₃₂₆ (Supplementary Figure S3D). Therefore, the RasGAP-derived peptide does not require the endogenous wild-type molecule (i.e., RasGAP) to mediate its cellular effects on adhesion.

Integrins and CD44 adhesion receptors are not required for TAT-RasGAP₃₁₇₋₃₂₆-mediated increased cell adhesiveness

We investigated whether TAT-RasGAP₃₁₇₋₃₂₆ requires integrin functions. Integrins are heterodimers composed of one α and one β subunit. There are 18 different known α and β subunits that can combine to form 24 different heterodimers.⁹ About 70% (16 out of 24) of these integrin dimers are made of either the α_V - or the $\beta 1$ -integrins (Supplementary Figure S4A). The fact that a melanoma cell line deficient in α_V -integrin expression²⁶ was rendered more adherent by TAT-RasGAP₃₁₇₋₃₂₆ (Supplementary Figure S4B) together with the observation that $\beta 1$ -integrin silencing in HeLa cells did not prevent TAT-RasGAP₃₁₇₋₃₂₆ from triggering adherence (Supplementary Figure S4C) suggests, however, that these widespread integrins do not individually mediate the pro-adhesive phenotype induced by TAT-RasGAP₃₁₇₋₃₂₆. It is unlikely that other integrins are targeted by the RasGAP peptide to mediate its effects on adhesion for the following reasons: (i) $\beta 2$ -, $\beta 3$ -, $\beta 4$ - and $\beta 7$ -integrins are expressed at very low levels or are not detected in U2OS cells (Supplementary Figure S4D)²⁷ that are responsive to TAT-RasGAP₃₁₇₋₃₂₆; (ii) the

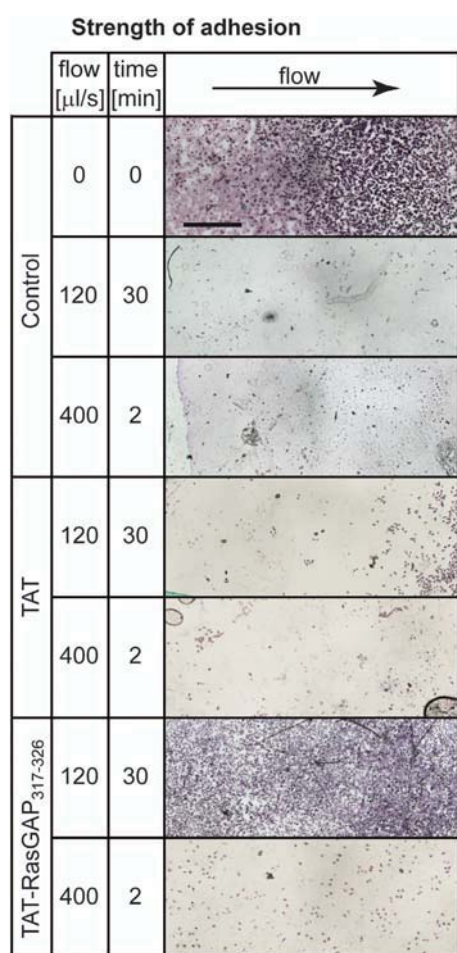


Figure 2. TAT-RasGAP₃₁₇₋₃₂₆ increases anchorage strength of cells to their substratum. HeLa cells were plated on gelatin-coated coverslips and were treated for 16 h with 20 μM TAT, TAT-RasGAP₃₁₇₋₃₂₆ or left untreated. They were then subjected to a flow-mediated detachment assay. The images shown are representative and display the cells after a detachment provoked by an intermediate strength flow (120 $\mu\text{l/s}$) or by an intense flow (400 $\mu\text{l/s}$) on a cell-occupied surface of 20 mm^2 in a chamber volume of 40 mm^3 . Scale bar: 100 μm .

expression of β 2- and β 7-integrin is usually restricted to immune cells.²⁸ We also tested the involvement of the CD44 glycoprotein, a FA-independent adhesion receptor that can also interact with ECM.²⁹ However, upon CD44 silencing in HeLa cells, TAT-RasGAP₃₁₇₋₃₂₆ could still increase adhesion (Supplementary Figure S4E). Consistent with our results on integrins are the data showing that TAT-RasGAP₃₁₇₋₃₂₆-mediated adhesion does not occur through a specific ECM as cell adhesion to collagen, fibronectin and laminin was increased by the RasGAP peptide (Supplementary Figure S4F). Altogether, the results indicate that CD44, β 1-integrin and α_v -integrin are individually dispensable for the adhesion-activating effect of TAT-RasGAP₃₁₇₋₃₂₆.

TAT-RasGAP₃₁₇₋₃₂₆ remodels FAs and induces actin depolymerization

FAs are protein complexes through which the cytoskeleton is connected to the extracellular matrix and as such could be modulated by TAT-RasGAP₃₁₇₋₃₂₆ to increase cell adhesion. Focal adhesion kinase (FAK), when recruited to activated integrins, acts as a key protein during FA formation and turnover. For example, it regulates the dynamics of actin fibers by favoring actin polymerization through phosphorylation of N-WASP,

actin contraction via activation of p190 RhoGEF and actin fiber fluidity by phosphorylating α -actinin and inhibiting its actin cross-linking capacity.³⁰ Even though FAK-null cells are still able to form FAs, FAK recruitment to integrins remains a typical feature of FA formation and subsequent attachment to the actin cytoskeleton.^{30,31} To assess FA modulation and actin polymerization upon TAT-RasGAP₃₁₇₋₃₂₆ treatment, U2OS cells were labeled with antibodies specific for FAK, phospho-Tyr³⁹⁷-FAK or stained for filamentous actin (F-actin). A marked increase in cortical actin fibers forming peripheral concentric arc-like structures (Figure 3a; white arrows) was induced by the RasGAP-derived peptide, whereas stress fibers almost completely disappeared (Figure 3a; yellow arrows). Unexpectedly, the overall number of FAs decreased, and there was a redistribution of FAs to the cell periphery. In addition, TAT-RasGAP₃₁₇₋₃₂₆ treatment resulted in significant dephosphorylation of FAK at tyrosine 397, which indicates a reduction in FA turnover.³² The expression levels of the FA-associated FAK and vinculin proteins, or the cytoskeletal β -actin and α -tubulin, were not affected by the RasGAP-derived peptide (Figure 3b). The α -tubulin network was also not affected by TAT-RasGAP₃₁₇₋₃₂₆ (data not shown). Figure 3c shows that, using FAK knockout MEFs, the absence of FAK did not prevent

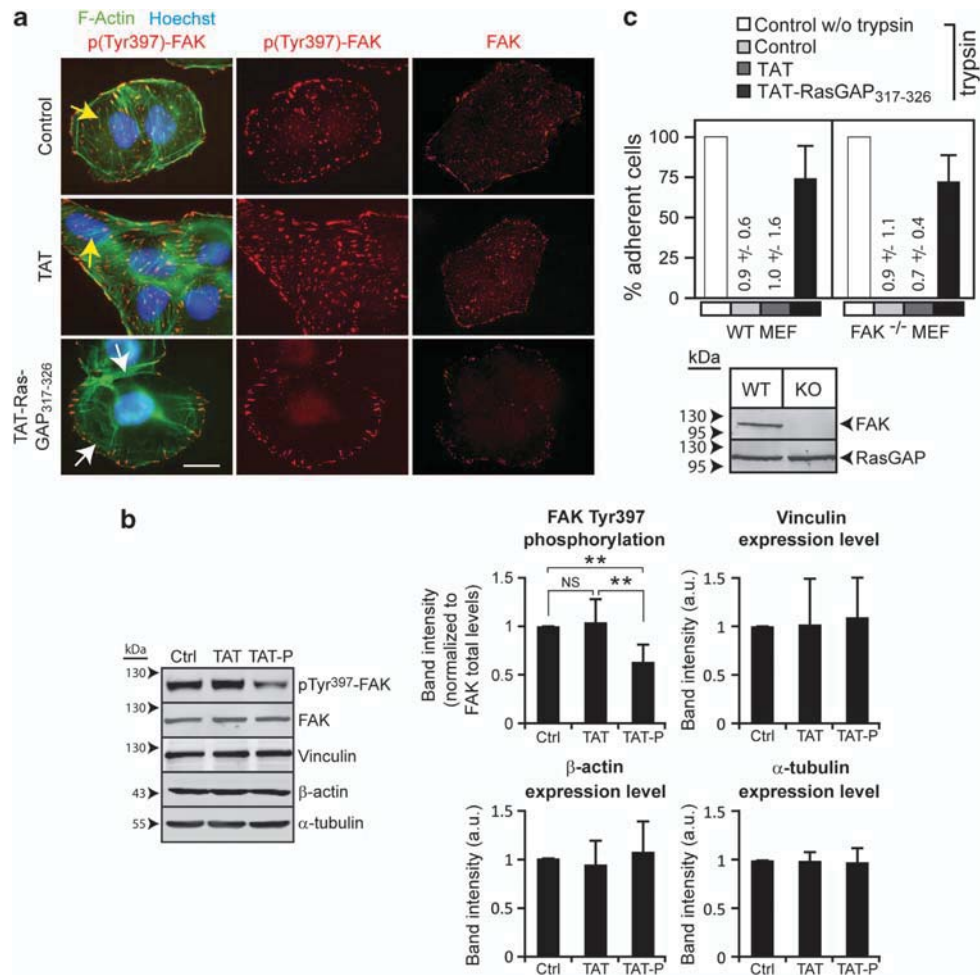


Figure 3. TAT-RasGAP₃₁₇₋₃₂₆ remodels actin cytoskeleton and focal adhesions. **(a)** U2OS cells were treated 16 h with 20 μ M TAT, TAT-RasGAP₃₁₇₋₃₂₆ or left untreated. Immunohistochemical staining against FAK and its phosphorylated form on tyrosine 397 (in red) was then performed. The F-actin cytoskeleton was stained with fluorescent phalloidin (in green), and nuclei were stained with Hoechst-33342 (in blue). Yellow arrows point at stress fibers and white arrows at cortical actin fibers. Scale bar: 10 μ m. **(b)** U2OS cells were treated 16 h with 20 μ M TAT, TAT-RasGAP₃₁₇₋₃₂₆ (TAT-P) or left untreated (Ctrl). The expression of the indicated proteins was assessed by western blotting. Representative images and quantifications are shown ($n=6$ independent experiments) **(c)**. Wild-type MEFs or FAK^{-/-} MEFs were treated for 8 h with 20 μ M TAT, TAT-RasGAP₃₁₇₋₃₂₆ or left untreated, and a trypsin-mediated detachment assay was performed. FAK expression was checked by immunoblotting. Values too low to be seen on the figure graphs are shown literally.

TAT-RasGAP₃₁₇₋₃₂₆ to increase adherence, excluding FAK as being the target of the RasGAP-derived peptide.

Because TAT-RasGAP₃₁₇₋₃₂₆-treated cells exhibited a loss of stress fibers, the effect of the peptide on actin fiber dynamics was investigated by measuring the ratio between polymerized F-actin and monomeric G-actin. Figure 4a shows that the F/G-actin ratio was significantly decreased upon TAT-RasGAP₃₁₇₋₃₂₆ treatment to values similar as those obtained when known actin inhibitors (latrunculin A and cytochalasin D) were used. Interestingly, similar to TAT-RasGAP₃₁₇₋₃₂₆, both latrunculin A and cytochalasin D increased cell adhesion, whereas jasplakinolide, an actin polymerization inducer, did not (Figure 4b). This suggests that actin depolymerization is involved in TAT-RasGAP₃₁₇₋₃₂₆-mediated cell adhesion increase. An *in vitro* pyrene-actin-based polymerization assay revealed, however, that RasGAP₃₁₇₋₃₂₆ alone does not slow down actin polymerization (Figure 4c), indicating that TAT-RasGAP₃₁₇₋₃₂₆-mediated actin depolymerization in cells is indirect.

TAT-RasGAP₃₁₇₋₃₂₆ does not require the Rho/ROCK axis to increase cell adhesiveness

As the SH3 domain of RasGAP has been shown to remodel the actin cytoskeleton in a Rho-dependent manner,³³ we investigated whether the activity of Rho could be modulated by the RasGAP-derived peptide. The level of the active GTP-bound RhoA, the main Rho family member, was assessed by performing a pull-down assay using the Rho-binding domain (RBD) of the Rhotekin protein that specifically binds to GTP-RhoA.³⁴ TAT-RasGAP₃₁₇₋₃₂₆-pretreated cells exhibited a significantly higher peak of Rho activation after 1 min of serum exposure (Figure 5a). These results show that, albeit only transiently, TAT-RasGAP₃₁₇₋₃₂₆ modulates Rho activation. RasGAP and p190RhoGAP have been previously

reported to form a complex, the biological relevance of which is thought to coordinate Ras- and Rho-mediated signaling pathways.³⁵ The possibility that TAT-RasGAP₃₁₇₋₃₂₆ disrupts this complex was evaluated. Supplementary Figure S5 shows that the RasGAP-RhoGAP interaction was not modulated by the RasGAP peptide, suggesting that the increase in RhoA activity by TAT-RasGAP₃₁₇₋₃₂₆ was not modulated at this level. This result is also consistent with the fact that the RasGAP-derived peptide does not require full-length RasGAP to mediate its effects (see Supplementary Figure S3D).

To further understand whether the TAT-RasGAP₃₁₇₋₃₂₆-mediated transient RhoA activation was needed for the increase in cell adherence, a trypsin-mediated detachment assay was performed in the absence or in the presence of the *Botulinum* C3 exoenzyme Rho inhibitor or Y-27632, an inhibitor of ROCK, an effector of Rho. Treatment with both drugs did not prevent TAT-RasGAP₃₁₇₋₃₂₆ from increasing adherence, indicating that this peptide does not mediate an increase in adhesion through activation of the Rho-ROCK pathway (Figure 5b). TAT-RasGAP₃₁₇₋₃₂₆ also prevented cell shrinking/rounding induced by the C3 exoenzyme (Figure 5c), a possible consequence of its capacity to increase adhesiveness.

TAT-RasGAP₃₁₇₋₃₂₆ impairs cell migration and invasion

It has been reported that a strong adhesion of cells to their substratum correlates with poor migration.³⁶ These observations raise the possibility that TAT-RasGAP₃₁₇₋₃₂₆ affects cell migration. Scratch wound healing assays were used to evaluate this assumption. Four different cancer and non-cancer cell lines (U2OS, HCT116, HeLa and HaCaT) were wounded and simultaneously treated or not with the TAT or TAT-RasGAP₃₁₇₋₃₂₆ peptides. A 48 h period of time was sufficient for untreated and

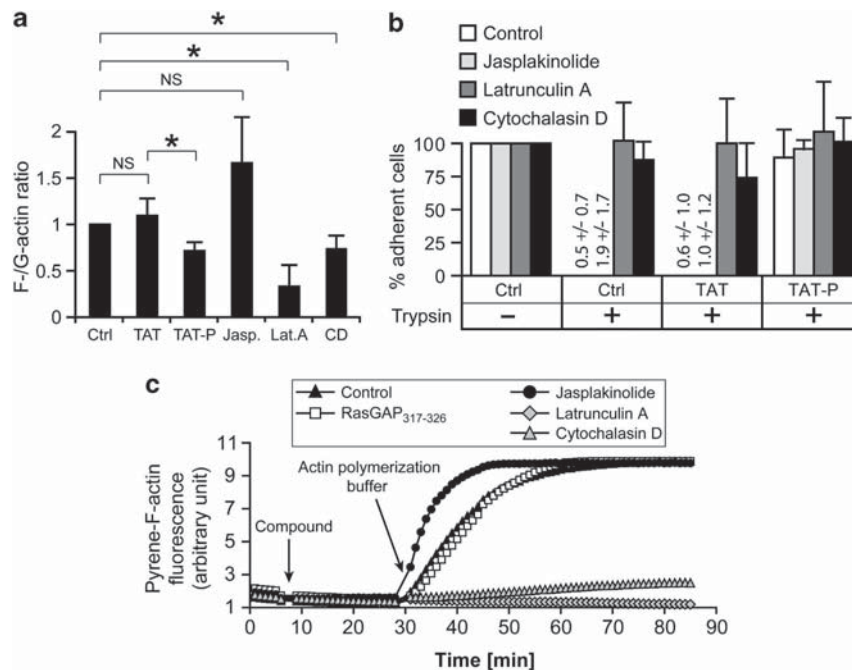


Figure 4. TAT-RasGAP₃₁₇₋₃₂₆ depolymerizes actin and actin depolymerization-inducing agents increase adherence. (a) U2OS cells were treated for 16 h with 50 nM of the actin polymerization promoter jasplakinolide (Jasp), with 500 nM of latrunculin A (Lat.A) and 5 μM cytochalasin D (CD), which are both actin depolymerization agents, together with 20 μM TAT, TAT-RasGAP₃₁₇₋₃₂₆ (TAT-P) and left untreated (Ctrl). An amount of 10 μg of Triton-insoluble (F-actin containing) and Triton-soluble (G-actin containing) fractions were subjected to a western blot directed against β-actin. The histogram shows the ratio between F-actin and G-actin. (b) U2OS cells were pre-treated for 1 h with 50 nM jasplakinolide, 500 nM latrunculin A, 5 μM cytochalasin D or were left untreated. They were then stimulated or not for 16 h with 20 μM TAT or TAT-RasGAP₃₁₇₋₃₂₆. A trypsin-mediated detachment assay was finally performed. Values too low to be seen on the figure graphs are shown literally. (c) An *in vitro* pyrene-actin polymerization assay was performed to evaluate the ability of RasGAP₃₁₇₋₃₂₆ to modulate actin polymerization by itself. Eight minutes after the beginning of the experiment, 20 μM RasGAP₃₁₇₋₃₂₆, 2 μM jasplakinolide, 6 μM latrunculin A or 6 μM cytochalasin D was added to the actin-containing buffer, followed 20 min later with the addition of the actin polymerization buffer. The graph shown is representative of five independent experiments.

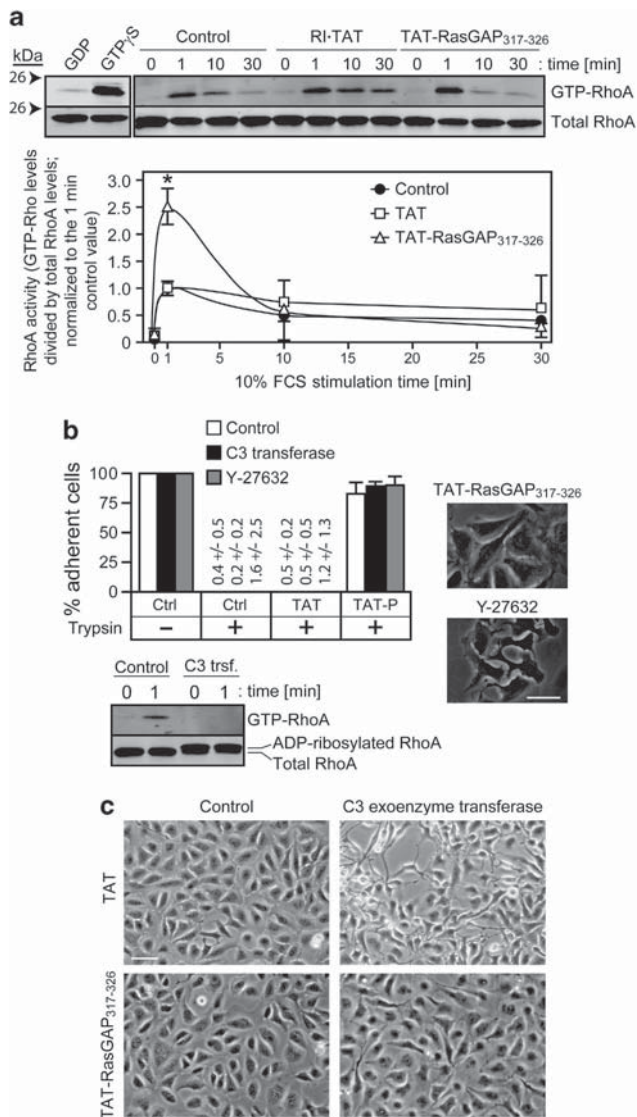


Figure 5. TAT-RasGAP₃₁₇₋₃₂₆ does not require the Rho/ROCK axis. (a) U2OS cells were treated 16 h with 20 μ M TAT, TAT-RasGAP₃₁₇₋₃₂₆ or left untreated and were then subjected to a RhoA activation assay (the statistical significance of the observed differences was assessed by one-way ANOVA). (b) U2OS cells were treated with the indicated combinations of 20 μ M TAT, 20 μ M TAT-RasGAP₃₁₇₋₃₂₆, 10 μ M of the Y-27632 ROCK inhibitor and 0.5 μ g/ml of the exoenzyme C3 transferase for 8 h. The cells were then subjected to a trypsin-mediated detachment assay (graph on the upper left of the panel). The two pictures on the right highlight the phenotype difference between TAT-RasGAP₃₁₇₋₃₂₆⁻ and Y-27632-treated cells (scale bar: 50 μ m). A RhoA activation assay was performed to control the inhibitory activity of the C3 transferase (blot on the lower left of the panel). Values too low to be seen on the figure graphs are shown literally. (c) U2OS cells were pre-incubated 1 h with 0.5 μ g/ml exoenzyme C3 transferase or left untreated (Control) and then treated with 20 μ M TAT or TAT-RasGAP₃₁₇₋₃₂₆ for 12 additional hours. Bright-field pictures are shown. Scale bar: 50 μ m.

TAT-only treated cells to fill the wounds entirely, whereas TAT-RasGAP₃₁₇₋₃₂₆-treated cells exhibited highly impaired motility (Figure 6a; time-lapse movie in Supplementary Material). This observation was further confirmed using a transwell Boyden chamber migration assay in which TAT-RasGAP₃₁₇₋₃₂₆ recapitulated the inhibition on cell migration (Figure 6b). Because RasGAP modulates cell proliferation through Ras, we assessed whether

TAT-RasGAP₃₁₇₋₃₂₆ affects cell proliferation to rule out the possibility that impaired migration was a consequence of decreased proliferation. However, the peptide did not impair proliferation of adherent cells (Supplementary Figure S6A) or cells in suspension (Supplementary Figure S6B). These results were confirmed by testing the ability of U2OS cells to incorporate radioactive thymidine in the presence of TAT-RasGAP₃₁₇₋₃₂₆ (Supplementary Figure S6C). As migration is a hallmark of invasiveness, we tested whether TAT-RasGAP₃₁₇₋₃₂₆ could hamper cell invasion. Using a transwell Boyden chamber layered with an extracellular matrix gel, it was found that TAT-RasGAP₃₁₇₋₃₂₆ also prevented invasion of MDA-MB-231 cells (Figure 6C).

DLC1 is required for TAT-RasGAP₃₁₇₋₃₂₆-mediated migration inhibition

Several RasGAP binding partners have been identified in the past.¹⁷ Among them, DLC1, a RhoGAP with tumor and metastasis suppressor activities, binds the SH3 domain of RasGAP via its GAP domain.^{14,37} The reported consequence of this binding is an inhibition of the DLC1 RhoGAP activity and impairment of its oncosuppressive activity. Fragment N2, the RasGAP₃₁₇₋₃₂₆-containing polypeptide that is physiologically generated by high levels of caspase-3²³ and that increases cell adhesion (Supplementary Figure S2C) was also able to interact with DLC1 (Figure 7a). However, an alanine substitution of tryptophan 317, an evolutionarily conserved residue within the RasGAP₃₁₇₋₃₂₆ sequence, abrogated the ability of fragment N2 to bind to DLC1 (Figure 7a). A TAT-RasGAP₃₁₇₋₃₂₆ peptide version bearing the W317A mutation failed to increase cell adherence (Figure 7b). These results indicate that the interaction of tryptophan 317 with DLC1 is essential for TAT-RasGAP₃₁₇₋₃₂₆-mediated effects on cell adhesiveness.

The involvement of DLC1 in the pro-adhesion and anti-migratory functions of TAT-RasGAP₃₁₇₋₃₂₆ was assessed in DLC1 knockout MEFs. In contrast to wild-type MEFs, DLC1-null MEFs were efficiently detached by trypsin despite the presence of TAT-RasGAP₃₁₇₋₃₂₆ (Figure 7c). Moreover, TAT-RasGAP₃₁₇₋₃₂₆ did not, or only minimally, hamper migration of DLC1-null cells, in contrast again to wild-type MEFs that were unable to migrate into wounds in the presence of the peptide (Figure 7d). To exclude the possibility that the inability of the DLC1 knockout MEFs to respond to TAT-RasGAP₃₁₇₋₃₂₆ was caused by something else than the absence of DLC1, the DLC1-null cells were transfected with a DLC1-encoding plasmid together with a GFP-encoding plasmid to label and track the transfected cells. Figure 7e shows that the transfected cells, in contrast to the non-transfected ones, were markedly impaired in the ability to migrate into wounds in the presence of TAT-RasGAP₃₁₇₋₃₂₆. Altogether, these experiments demonstrate that the RasGAP-derived peptide requires DLC1 to exert its pro-adhesion and anti-migratory activities.

DISCUSSION

Blocking invasion is a prime strategy to inhibit the initial steps of the metastatic dissemination. In this study, we found that TAT-RasGAP₃₁₇₋₃₂₆, previously shown to sensitize cancer cells to various anticancer treatments,¹⁹⁻²¹ potently inhibits cell migration and invasion by targeting the DLC1 tumor suppressor.

Earlier reports have indicated that RasGAP can control cell migration. RasGAP knockout MEFs exhibit reduced migration, whereas RasGAP silencing in breast cancer cells enhances their motility.^{38,39} These conflicting results could be a consequence of the different cellular systems investigated. Another possibility is that the dosage of RasGAP reduction influences the resulting effect on migration. It can be envisioned that RasGAP both positively and negatively regulates cell migration, possibly in response to different stimuli, but that the negative regulation requires high level of expression of the protein. In this case, the

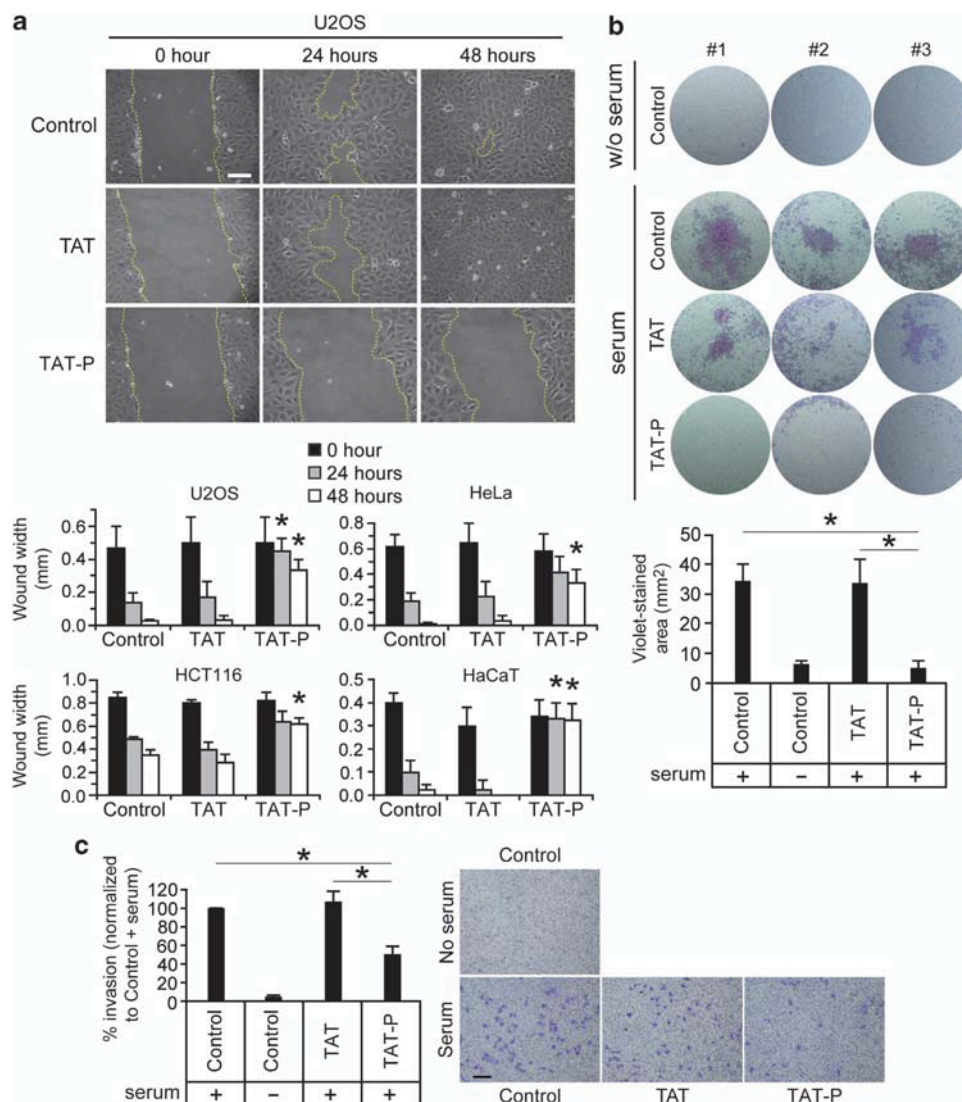


Figure 6. TAT-RasGAP₃₁₇₋₃₂₆ inhibits cell migration and invasion. **(a)** The indicated cell lines were subjected to wound-healing scratch assays. After wounding, the cells were left untreated or incubated 24 and 48 hours with 20 μ M TAT or TAT-RasGAP₃₁₇₋₃₂₆. Wound widths at the indicated time are reported in the graphs ($n=4$ independent experiments). Scale bar: 100 μ m. **(b)** 4T1 cells were cultured in the upper chamber of transwell plates and allowed to migrate through the Transwell filters for 24 h in the absence (control) or in the presence of 20 μ M TAT or TAT-RasGAP₃₁₇₋₃₂₆. DMEM complemented (+) or not (-) with serum was added in the lower chamber. Quantitation was done as described in the methods. Three representative independent images are shown per condition. **(c)** MDA-MB-231 cells were allowed to invade the Matrigel matrix by following a serum gradient for 48 h in the presence of 20 μ M TAT or TAT-RasGAP₃₁₇₋₃₂₆. A negative control without serum in the lower chamber was also performed. The invading cells were then counted and expressed as the percentage of invading cells per transwell over the 'control + serum' condition. Representative images are shown. Scale bar: 50 μ m.

reduction in RasGAP levels could favor cell migration. The observation that overexpression of RasGAP fragments correlates with decreased adherence⁴⁰ is consistent with this notion. In contrast, complete absence of RasGAP expression, as is the case in knockout cells, would remove any positive effect of RasGAP on cell migration. However, the ability of TAT-RasGAP₃₁₇₋₃₂₆ to inhibit cell migration does not involve a modulation of the full-length RasGAP protein as the peptide also blocks cell migration in RasGAP knockout cells (Supplementary Figure S3). It is therefore likely that if full-length RasGAP and TAT-RasGAP₃₁₇₋₃₂₆ use the same pathway to regulate cell adhesion, it is a consequence of targeting the same molecules and not the result of the peptide modulating the activity of the parental RasGAP protein.

The SH3 domain of RasGAP can reorganize actin cytoskeleton in a Rho-dependent manner,^{33,38} presumably via the recruitment of

p190RhoGAP.^{35,38} TAT-RasGAP₃₁₇₋₃₂₆ can also favor Rho activation, at least transiently (Figure 5), but this apparently is not required for its capacity to increase cell adherence as inhibition of Rho or the Rho effector ROCK does not affect TAT-RasGAP₃₁₇₋₃₂₆-mediated cell adhesiveness increase.

Although α_V - and β_1 -integrins were not individually required, TAT-RasGAP₃₁₇₋₃₂₆ may nevertheless exert its effects through FA modulation. Rac-induced formation of nascent FAs can generate huge adhesive forces,¹¹ raising the hypothesis that the RasGAP-derived peptide prevents FA maturation, therefore retaining FAs in their hyper-adherent state. Consistent with this hypothesis are the observations that TAT-RasGAP₃₁₇₋₃₂₆ induced FAK dephosphorylation and relocation of FAs to the cell periphery (Figure 3), which is typical of FA turnover inhibition.¹¹ The involvement of other adhesion receptors in

actin depolymerization and inhibition of migration. This would also induce peripheral FA redistribution,³² a phenotype that is seen in TAT-RasGAP₃₁₇₋₃₂₆-treated cells (Figure 3). The fact that displacing DLC1 from FAs, through abrogation of FAK and tensin binding, does not affect the DLC1 RhoGAP activity⁴² is consistent with our observation that Rho activity is not markedly modulated by TAT-RasGAP₃₁₇₋₃₂₆ (Figure 5).

DLC1 may not be the only target of the RasGAP-derived peptide as some residual attachment was observed in TAT-RasGAP₃₁₇₋₃₂₆-treated DLC1-null MEFs (Figure 7). For example, proteins sharing redundancy with DLC1, such as DLC2 and DLC3, may partially compensate for the lack of DLC1. The involvement of such proteins in TAT-RasGAP₃₁₇₋₃₂₆ functions remains to be investigated.

The present study identifies TAT-RasGAP₃₁₇₋₃₂₆ as an activator of cell adhesion and an inhibitor of cell migration and invasion. Earlier work has shown that this RasGAP-derived peptide increases the death of tumor cells induced by various anticancer treatments.¹⁹⁻²¹ Therefore, TAT-RasGAP₃₁₇₋₃₂₆ could exert two beneficial effects as an anticancer agent, first by increasing the sensitivity of tumor cells to anticancer drugs and second by reducing the invasive potential of tumor cells.

MATERIALS AND METHODS

Cell lines, cell culture and transfection

All cell lines were cultured at 37 °C and in 5% CO₂. U2OS, 4T1, HCT116, SAOS, 3T3, RasGAP-null, FAK-null and DLC1-null MEFs, M21 (α_V -integrin null), M21L (α_V -integrin positive), MDA-MB-231-Luc and 293T cells were maintained in Dulbecco's modified Eagle Medium (DMEM) (Gibco, Paisley, UK) supplemented with 10% fetal bovine serum (FBS) (Gibco). HeLa and Jurkat cells were maintained in RPMI 1640 (Gibco) supplemented with 10% FBS. HaCaT cells were maintained in keratinocyte medium (Invitrogen, Carlsbad, CA, USA). The 293T cells were transfected using the calcium-phosphate method.^{19,44} MEFs were transfected using the Lipofectamine 2000 reagent (Invitrogen) according to the manufacturer's instructions.

Antibodies

The antibodies used were obtained from the following sources (their dilution and specific buffer are described in the Supplementary methods): anti-c-Myc, anti-FAK, anti-phospho-Tyr³⁹⁷-FAK and anti-RhoA (Cell Signaling, Danvers, MA, USA); anti-vinculin (Sigma-Aldrich, St Louis, MO, USA); anti- β -actin (Chemicon, Billerica, MA, USA); anti- α -tubulin (Serotec, Raleigh, NC, USA); anti-RasGAP (Enzo life sciences, Farmingdale, NY, USA); anti-CD44 (Abcam, Cambridge, UK); anti- β 1-integrin (BD Pharmingen, San Jose, CA, USA); anti-V5 (Invitrogen); and anti-HA (Covance, Princeton, NJ, USA). The secondary antibodies were IRDye800-conjugated anti-mouse IgG and IRDye800-conjugated anti-rabbit IgG (Rockland, Gilbertsville, PA, USA), AlexaFluor680-conjugated anti-mouse IgG and AlexaFluor680-conjugated anti-rabbit IgG (Molecular Probes, Paisley, UK) and donkey Cy-anti-rabbit antibody (Jackson ImmunoResearch, West Grove, PA, USA; for immunocytochemistry).

Peptide synthesis and treatment and plasmids

All peptides are described and were synthesized as previously reported.¹⁹ The R9 and R9-RasGAP₃₁₇₋₃₂₆ peptides were kind gifts from Dr Christoph Kündig (MedDiscovery, Geneva, Switzerland). Plasmid description is detailed in the Supplementary Methods.

Detachment assay

Cells were cultured until 80% confluence was reached and were treated as indicated in the figures. After a phosphate-buffered saline (PBS) wash, the non-trypsinized cells were directly colored with the Giemsa stain. The other cells were incubated with 5 g/l trypsin, 15 mM EDTA solution or with trypsin/EDTA (5 g/l trypsin, 6.8 mM EDTA) for 5 min. The cells were then washed once with phosphate-buffered saline and colored with the Giemsa stain. Four pictures per plate were taken using a Zeiss Axioplan 2 microscope equipped with a 10 × objective. The number of adherent cells was then counted for each picture and expressed as the number of cells per mm² or alternatively as the percentage of adherent cells over the

non-trypsinized control. The flow-mediated detachment assay is precisely described in the Supplementary Methods.

Adhesion assay

U2OS cells were allowed to adhere with the indicated compounds for the indicated periods of time. The medium was then aspirated and the cells were gently washed once with phosphate-buffered saline and colored with the Giemsa stain. The data were collected as for detachment assays.

Western blot analysis

Cells were treated as indicated in the figures and western blots were performed as previously described.¹⁹ Unless otherwise mentioned, 40 μ g of proteins were loaded.

Wound-healing scratch assay, transwell migration and invasion assays

Wound-healing scratch assays were performed as described earlier⁴⁵ and details are described in the Supplementary Methods. For the transwell migration assay, 50,000 overnight-starved 4T1 cells were seeded in the upper chamber of 24 transwell plates (Corning, Corning, NY, USA) for 2.5 h. The cells were then subjected to the treatments indicated in the figures for 3 h. DMEM complemented or not with 10% FBS was then placed in the lower chamber of the transwell plates, and the cells were allowed to migrate for 24 h. Cells that migrated through the filters were quantified as described in the Supplementary Methods.

For the transwell invasion assay, overnight-starved MDA-MB-231-luc cells were pre-treated for 2 h with 20 μ M TAT, 20 μ M TAT-RasGAP₃₁₇₋₃₂₆ or left untreated. A total of 5000 cells were resuspended in 100 μ l of 4 mg/ml Matrigel (BD Biosciences, San Jose, CA, USA) complemented or not with 20 μ M TAT, 20 μ M TAT-RasGAP₃₁₇₋₃₂₆, and placed in the top chamber. DMEM complemented or not with 10% FBS was then placed in the bottom chamber, and the cells were allowed to migrate through the filter for 48 h. The crystal-violet-colored invading cells were then counted for each condition and the results were expressed as the percentage of invading cells per transwell over the 'control + serum' condition.

Statistical analysis

Unless otherwise mentioned, all experiments were performed three times and independently. The results were always expressed as mean \pm 95% confidence intervals. Unless otherwise mentioned, Student's *t*-tests were performed to assess significant differences and using the appropriate Microsoft Excel function. The Bonferroni correction was applied when more than one comparison was performed. One-way and repeated-measurement ANOVAs were performed using the R software (Vienna, Austria; version 2.11.0) and were followed by a Tukey test for multiple comparisons. Asterisks denote statistical significant differences (*P*-value < 0.05).

CONFLICT OF INTEREST

CW is a co-inventor of the TAT-RasGAP₃₁₇₋₃₂₆ compound as an anti-tumor agent (patent owned by the University of Lausanne) and may receive royalties from patent licensing if the compound is commercialized.

ACKNOWLEDGEMENTS

This work was supported by a grant from Oncosuisse (KFS-02543-02-2010). We thank Professor Nicholas C. Popescu (National Cancer Institute, Bethesda) for the DLC1-null MEFs and Professor David Schlaepfer (Moores UCSD Cancer Center, La Jolla) for the FAK-null MEFs.

REFERENCES

- 1 Jemal A, Bray F, Center MM, Ferlay J, Ward E, Forman D. Global cancer statistics. *CA Cancer J Clin* 2011; **61**: 69–90.
- 2 Hanahan D, Weinberg RA. Hallmarks of cancer: the next generation. *Cell* 2011; **5**: 646–674.
- 3 Thiery JP. Epithelial-mesenchymal transitions in tumour progression. *Nat Rev Cancer* 2002; **6**: 442–454.
- 4 Yilmaz M, Christofori G. EMT, the cytoskeleton, and cancer cell invasion. *Cancer Metastasis Rev* 2009; **1-2**: 15–33.

- 5 Chiang AC, Massague J. Molecular basis of metastasis. *N Engl J Med* 2008; **26**: 2814–2823.
- 6 Sethi N, Kang Y. Unravelling the complexity of metastasis - molecular understanding and targeted therapies. *Nat Rev Cancer* 2011; **10**: 735–748.
- 7 Bravo-Cordero JJ, Hodgson L, Condeelis J. Directed cell invasion and migration during metastasis. *Curr Opin Cell Biol* 2012; **2**: 277–283.
- 8 Friedl P, Wolf K. Tumour-cell invasion and migration: diversity and escape mechanisms. *Nat Rev Cancer* 2003; **5**: 362–374.
- 9 Byron A, Morgan MR, Humphries MJ. Adhesion signalling complexes. *Curr Biol* 2010; **24**: R1063–R1067.
- 10 Raftopoulos M, Hall A. Cell migration: Rho GTPases lead the way. *Dev Biol* 2004; **1**: 23–32.
- 11 Geiger B, Bershadsky A, Pankov R, Yamada KM. Transmembrane crosstalk between the extracellular matrix–cytoskeleton crosstalk. *Nat Rev Mol Cell Biol* 2001; **11**: 793–805.
- 12 McClatchey AI, Giovannini M. Membrane organization and tumorigenesis—the NF2 tumor suppressor, Merlin. *Genes Dev* 2005; **19**: 2265–2277.
- 13 Aoki K, Taketo MM. Adenomatous polyposis coli (APC): a multi-functional tumor suppressor gene. *J Cell Sci* 2007; **120**: 3327–3335.
- 14 Durkin ME, Yuan BZ, Zhou X, Zimonjic DB, Lowy DR, Thorgeirsson SS *et al.* DLC-1: a Rho GTPase-activating protein and tumour suppressor. *J Cell Mol Med* 2007; **5**: 1185–1207.
- 15 Lahoz A, Hall A. DLC1: a significant GAP in the cancer genome. *Genes Dev* 2008; **13**: 1724–1730.
- 16 Yang X, Popescu NC, Zimonjic DB. DLC1 interaction with S100A10 mediates inhibition of in vitro cell invasion and tumorigenicity of lung cancer cells through a RhoGAP-independent mechanism. *Cancer Res* 2011; **8**: 2916–2925.
- 17 Pamonsinlapham P, Hadj-Slimane R, Lepelletier Y, Allain B, Toccafondi M, Garbay C *et al.* p120-Ras GTPase activating protein (RasGAP): a multi-interacting protein in downstream signaling. *Biochimie* 2009; **3**: 320–328.
- 18 Yang JY, Widmann C. Antiapoptotic signaling generated by caspase-induced cleavage of RasGAP. *Mol Cell Biol* 2001; **16**: 5346–5358.
- 19 Michod D, Yang JY, Chen J, Bonny C, Widmann C. A RasGAP-derived cell permeable peptide potently enhances genotoxin-induced cytotoxicity in tumor cells. *Oncogene* 2004; **55**: 8971–8978.
- 20 Michod D, Annibaldi A, Schaefer S, Dapples C, Rochat B, Widmann C. Effect of RasGAP N2 fragment-derived peptide on tumor growth in mice. *J Natl Cancer Inst* 2009; **11**: 828–832.
- 21 Pittet O, Petermann D, Michod D, Krueger T, Cheng C, Ris HB *et al.* Effect of the TAT-RasGAP(317–326) peptide on apoptosis of human malignant mesothelioma cells and fibroblasts exposed to meso-tetra-hydroxyphenyl-chlorin and light. *J Photochem Photobiol B* 2007; **1**: 29–35.
- 22 Barras D, Widmann C. Promises of apoptosis-inducing peptides in cancer therapeutics. *Curr Pharm Biotechnol* 2011; **8**: 1153–1165.
- 23 Yang JY, Walicki J, Michod D, Dubuis G, Widmann C. Impaired Akt activity down-modulation, caspase-3 activation, and apoptosis in cells expressing a caspase-resistant mutant of RasGAP at position 157. *Mol Biol Cell* 2005; **8**: 3511–3520.
- 24 Karaman MW, Herrgard S, Treiber DK, Gallant P, Atteridge CE, Campbell BT *et al.* A quantitative analysis of kinase inhibitor selectivity. *Nat Biotechnol* 2008; **1**: 127–132.
- 25 Ross B, Kristensen O, Favre D, Walicki J, Kastrop JS, Widmann C *et al.* High resolution crystal structures of the p120 RasGAP SH3 domain. *Biochem Biophys Res Commun* 2007; **2**: 463–468.
- 26 Felding-Habermann B, Mueller BM, Romerdahl CA, Cheresch DA. Involvement of integrin alpha V gene expression in human melanoma tumorigenicity. *J Clin Invest* 1992; **6**: 2018–2022.
- 27 Beck M, Schmidt A, Malmstroem J, Claassen M, Ori A, Szymborska A *et al.* The quantitative proteome of a human cell line. *Mol Syst Biol* 2011; **7**: 549.
- 28 Sheppard D. In vivo functions of integrins: lessons from null mutations in mice. *Matrix Biol* 2000; **3**: 203–209.
- 29 Ponta H, Sherman L, Herrlich PA. CD44: from adhesion molecules to signalling regulators. *Nat Rev Mol Cell Biol* 2003; **1**: 33–45.
- 30 Mitra SK, Hanson DA, Schlaepfer DD. Focal adhesion kinase: in command and control of cell motility. *Nat Rev Mol Cell Biol* 2005; **1**: 56–68.
- 31 Ilic D, Furuta Y, Kanazawa S, Takeda N, Sobue K, Nakatsuji N *et al.* Reduced cell motility and enhanced focal adhesion contact formation in cells from FAK-deficient mice. *Nature* 1995; **6549**: 539–544.
- 32 Hamadi A, Bouali M, Dontenwill M, Stoeckel H, Takeda K, Ronde P. Regulation of focal adhesion dynamics and disassembly by phosphorylation of FAK at tyrosine 397. *J Cell Sci* 2005; **118**: 4415–4425.
- 33 Leblanc V, Tocque B, Delumeau I. Ras-GAP controls Rho-mediated cytoskeletal reorganization through its SH3 domain. *Mol Cell Biol* 1998; **9**: 5567–5578.
- 34 Ren XD, Kiosses WB, Schwartz MA. Regulation of the small GTP-binding protein Rho by cell adhesion and the cytoskeleton. *EMBO J* 1999; **3**: 578–585.
- 35 Hu KQ, Settleman J. Tandem SH2 binding sites mediate the RasGAP-RhoGAP interaction: a conformational mechanism for SH3 domain regulation. *EMBO J* 1997; **3**: 473–483.
- 36 Palecek SP, Loftus JC, Ginsberg MH, Lauffenburger DA, Horwitz AF. Integrin-ligand binding properties govern cell migration speed through cell-substratum adhesiveness. *Nature* 1997; **6616**: 537–540.
- 37 Yang XY, Guan M, Vigil D, Der CJ, Lowy DR, Popescu NC. p120Ras-GAP binds the DLC1 Rho-GAP tumor suppressor protein and inhibits its Rho GTPase and growth-suppressing activities. *Oncogene* 2009; **11**: 1401–1409.
- 38 Kulkarni SV, Gish G, van der Geer P, Henkemeyer M, Pawson T. Role of p120 Ras-GAP in directed cell movement. *J Cell Biol* 2000; **2**: 457–470.
- 39 Mai A, Veltel S, Pellinen T, Padzik A, Coffey E, Marjomaki V *et al.* Competitive binding of Rab21 and p120RasGAP to integrins regulates receptor traffic and migration. *J Cell Biol* 2011; **2**: 291–306.
- 40 McGlade J, Brunkhorst B, Anderson D, Mbamalu G, Settleman J, Dedhar S *et al.* The N-terminal region of GAP regulates cytoskeletal structure and cell adhesion. *EMBO J* 1993; **8**: 3073–3081.
- 41 Kawai K, Yamaga M, Iwamae Y, Kiyota M, Kamata H, Hirata H *et al.* A PLC δ 1-binding protein, p122RhoGAP, is localized in focal adhesions. *Biochem Soc Trans* 2004; **32**: 1107–1109.
- 42 Li G, Du X, Vass WC, Papageorge AG, Lowy DR, Qian X. Full activity of the deleted in liver cancer 1 (DLC1) tumor suppressor depends on an LD-like motif that binds talin and focal adhesion kinase (FAK). *Proc Natl Acad Sci USA* 2011; **41**: 17129–17134.
- 43 Yin HL, Janmey PA. Phosphoinositide regulation of the actin cytoskeleton. *Annu Rev Physiol* 2003; **65**: 761–789.
- 44 Jordan M, Schallhorn A, Wurm FM. Transfecting mammalian cells: optimization of critical parameters affecting calcium-phosphate precipitate formation. *Nucleic Acids Res* 1996; **4**: 596–601.
- 45 Bulat N, Waeber G, Widmann C. LDLs stimulate p38 MAPKs and wound healing through SR-BI independently of Ras and PI3 kinase. *J Lipid Res* 2009; **1**: 81–89.

Supplementary Information accompanies this paper